JOURNAL OF SOLID STATE CHEMISTRY 48, 431–438 (1983)

The System Copper–Tellurium

R. BLACHNIK,* M. LASOCKA,† AND U. WALBRECHT

Anorganische Chemie, FB Chemie-Biologie der Universität-GH-Siegen, D-5900 Siegen 21, West Germany

Received November 8, 1982; in revised form March 21, 1983

The system copper–tellurium was investigated by DTA, DSC, and X-ray methods. A phase diagram with the phases $Cu_{2-x}Te$ (33.5–36.2 mole% Te), $Cu_{3-x}Te_2$ (40–41 mole%), and CuTe was constructed. In the homogeneity ranges of the nonstoichiometric phases several superstructures were observed. The lattice parameters and *d* values of some of these phases are given.

Introduction

The system Cu–Te given by Hansen (*1*) is rather complex, especially within the concentration range between 33 and 45 mole% Te. Two compounds observed in this region are known as the natural minerals weissite and rickardite, respectively. The existence of a third compound with the composition CuTe has been confirmed by Schubert *et al.* (*2*) and Anderko and Schubert (*3*). This compound is also known as the mineral vulcanite.

Different methods have been used to study the Cu–Te system. Based on metallographic, dilatometric, and X-ray examinations, Anderko *et al.* (*3*) have determined temperatures of transformation in the compound Cu_2Te, as well as the structure of both CuTe and Cu_4Te_3. Using microscopic and roentgenographic techniques, Patzak (*4*) has investigated the phase areas of the system at room temperature. Similar studies have been performed by Van Con and Rodot (*5*), Stevels (*6*), and Miyatani *et al.* (*7*). However, the results are not consistent in certain details. The differences relate not only to the structures, transformation temperatures, and homogeneity ranges of the compounds, but also to the position of the miscibility gap between Cu and Cu_2Te as well as to the eutectic on the Te-rich side of the system.

In the present study the system Cu–Te was reexamined over the full concentration range in steps of 5 mole%, between Cu_2Te and CuTe in steps of 1 mole%, and within the most controversial region of 33–38 at.% Te in steps of 0.1 mole%.

Experimental

The alloys were prepared from stoichiometric amounts of high purity elemental solids by encapsulating them under vacuum in quartz ampoules, melting in a flame, annealing for 3 days at 900°C and homogenizing for two months at 300°C. In the homogeneity region of $Cu_{2-x}Te$ 40 samples were annealed 10 K above the various transformation temperatures (400–600 K)

* To whom correspondence should be addressed.

† Permanent address: Institute for Materials Science and Engineering, Warsaw Technical University.

0022-4596/83 $3.00

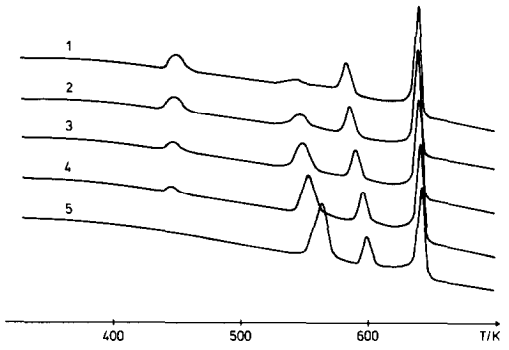

FIG. 1. DSC curves of five consecutive runs of $Cu_{2-x}Te$ (33.63 mole% Te).

and quenched to room temperature. The materials were subjected to systematic thermal analysis and X-ray studies.

The difference thermal analysis experiments were carried out using a DTA apparatus constructed in this laboratory (*8*), as well as with Du Pont 900 and Perkin–Elmer DSC-2 instruments, at a standard heating/cooling rate of 10 deg/min. Because of the rather complex nature of the effects, the DSC curves were also measured at very low scanning rate (0.31, 0.63, and 1.25 deg/min) to eliminate nonequilibrium effects. For individual samples a Calvet calorimeter (Setaram) was used at a heating/cooling rate of 0.167 deg/min.

Within the composition range of 36–46 mole% Te, some samples were investigated by microprobe analysis, using a Jeol Superprobe 733 unit. In these experiments special attention was paid to finding the homogeneity border for each of the coexisting phases in heterogeneous samples.

The DSC and DTA curves for some compositions within the homogeneity region of $Cu_{2-x}Te$ were affected by the thermal and mechanical history of the sample. The influence of the thermal treatment is illustrated in Fig. 1, which shows five consecutive runs for a sample with 33.63 mole% Te. The transitions below 650 K are strongly influenced. The DSC curves change gradually to another pattern, which was identified as the equilibrium curve of samples with a composition of ca. 34 mole% Te. After standing at room temperature for one month the original DSC curve was found in a new measurement.

Far more important was the effect of different mechanical treatment. These observations may explain some of the disagreeing results found in the literature. The DSC effects of the samples are changed with respect to peak area, peak temperature, and number of peaks where different grinding treatments using a ball mill with argon atmosphere are employed. The effect of mechanical treatment could also be observed in the corresponding X-ray patterns. The complicated patterns of equilibrated samples vanish. The lines appearing are very similar to the lines of the Nowotny phase (*9*).

Room-temperature X-ray analysis was carried out by means of a Guinier camera with Cu$K\alpha$ radiation. The lattice constants were determinated using AlSi as a standard and Cr$K\alpha$ radiation. A Simon–Guinier camera (Enraf-Nonius) with Cu$K\alpha$ radiation was used for the high-temperature X-ray studies. Heating rates of 10 or 5 deg per hr were chosen in most cases.

Results

On the basis of DTA and X-ray experiments a phase diagram for Cu–Te was constructed (Fig. 2). Some differences to the diagram previously reported by Hansen (*1*) were observed. For the miscibility gap on the metal-rich side not one but two lines were obtained, the upper one being the monotectic line at 1365 K and the lower, a eutectic line at 1323 K. Therefore, the miscibility gap lies on the primary crystallization area of Cu_2Te and at the temperatures below 1323 K secondary crystallization of Cu takes place. The boundaries of the miscibility gap were constructed using values of Burylev *et al.* (*10*). On the Te-rich side,

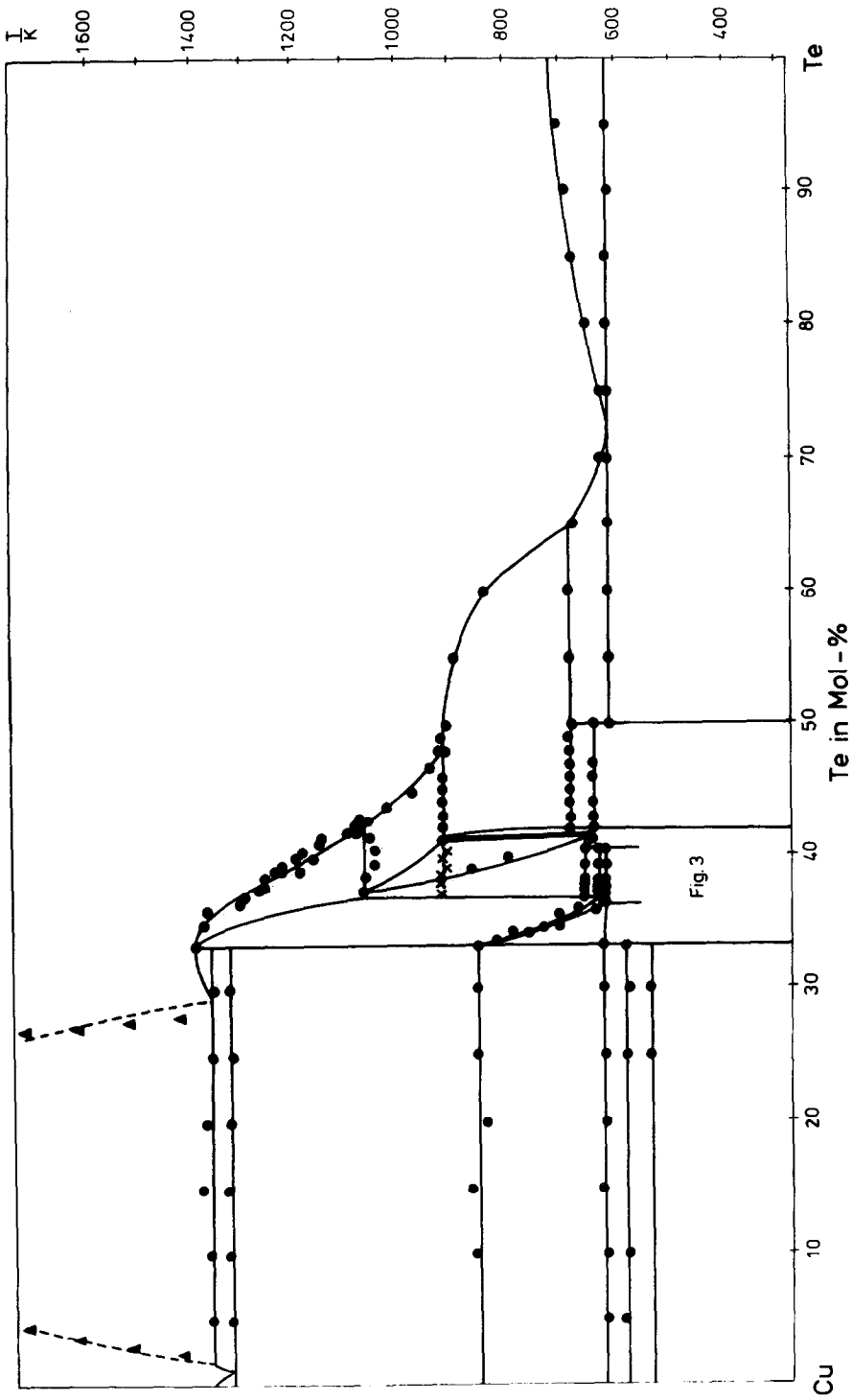

FIG. 2. Phase diagram of the system Cu–Te.

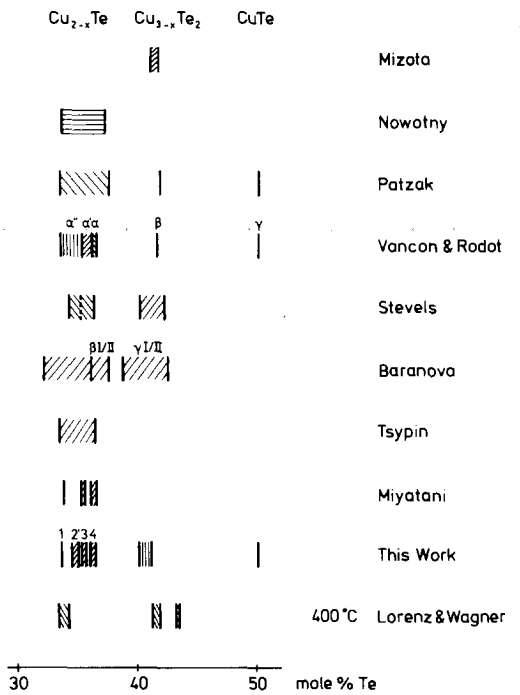

FIG. 3. The homogeneity ranges of the phases in the system Cu–Te.

not only was the stable Te–CuTe eutectic at 613 K observed but in addition all samples showed a metastable "Cu_3Te_2"–Te eutectic at 604 K. The latter is not shown in the diagram.

The composition range and structure of $Cu_{2-x}Te$ phases were studied intensively (Fig. 3). Nowotny (*9*) proposed a hexagonal structure and a homogeneity range for $Cu_{2-x}Te$, which was confirmed by Patzak (loc. cit.) and Schubert (loc. cit.). The latter papers report that at room temperature a hexagonal superstructure with lattice constants of $a' = 3a$ and $c' = 3c$ compared with the Nowotny phase is the stable modification of $Cu_{2-x}Te$.

The broad homogeneity range found by Patzak (*4*) was divided by some authors into several narrower ranges (Fig. 3) (*5–7*). For samples with these compositions, several structures or superstructures have been reported, which can be derived from a hexagonal subcell (*4–6, 9, 11, 12*). The occurrence of a particular structure depends on the composition and the thermal treatment. Stevels (*6*) reported previously that samples of composition $0 \leq x \leq 0.3$ were hexagonal (a = 4.14 Å, c = 7.25 Å) after rapid cooling from 700°C to room temperature. On holding the samples for a longer time at room temperature, some more complicated powder patterns were obtained as a function of time. A final equilibrium state was reached after four months.

Recently the phase diagram of $Cu_{2-x}Te$ ($x \leq 0.22$, T = 770 K) was established by Miyatani *et al.* (*7*) with the aid of coulometric titrations. The result agrees quite well with the diagram (Fig. 4) constructed from our DTA and X-ray measurements. The thermal effects are also confirmed by results given in the paper of Guastavino *et al.* (*13*), although Guastavino did not construct a phase diagram from his values.

Our results reveal that the $Cu_{2-x}Te$ phase extends from 33.5 to 36.2 mole% Te at 400 K.

The tellurium-rich side of $Cu_{2-x}Te$ is now probably correct. Between room temperature and 540 K a hexagonal phase (a = 8.328 Å, c = 7.219 Å, at 36.1 mole% Te, phase 4) exists. This phase is identical with the α phase of Van Con and Rodot (*5*), the *β-I* phase of Baranova (*11*), and the $Cu_{1.77}Te$ phase of Stevels. Between 550 and 615 K a new hexagonal phase (a = 8.453 Å, c = 21.793 Å, phase 3′) was found. This phase is the same as the phases *β*-II of Baranova (*11*), α' of Van Con *et al.* (*5*) and the hexagonal superstructure reported by Stevels for $Cu_{1.77}Te$. The 4–3′ transition is according to Baranova, an order–disorder transformation. Above 630 K we observed a two-phase region consisting of a hexagonal (a = 4.20 Å, c = 7.26 Å, phase 8) and a cubic phase (a = 6.03 Å, phase 9). The former phase is stable only up to ~660 K.

In the region from 34.9 to 35.9 mole% Te an X-ray pattern very similar to that of

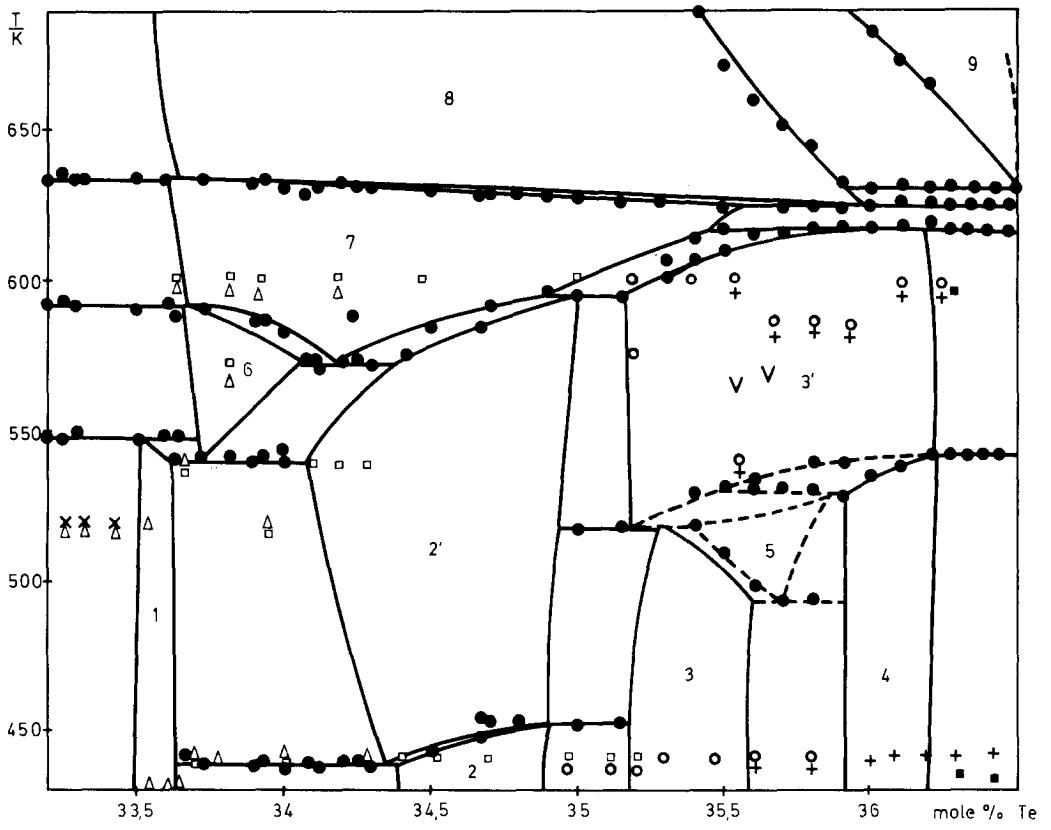

FIG. 4. Phase boundaries within the homogeneity range of $Cu_{2-x}Te$. x = Cu, △ = phase 1, □ = phase 2, ○ = phase 3, + = phase 4, ■ = Rickardit, V = phase 5? (in samples quenched from this temperature).

phase 3′ was observed. The lattice constants of this phase 3 are a = 8.378 Å, c = 10.877 Å at 35.3 mole% Te, in good agreement with those of a phase reported by Tsypin *et al.* (*14*) with a = 8.36 Å, c = 21.63 Å, ($\sim 2c$) at 35.2 mole%. Whether this phase is in fact the high-temperature phase 3′ is not clear, though some DSC measurements seem to exclude this possibility.

It was very difficult to identify the different superstructures at higher temperatures, as weak lines in the room-temperature Guinier photographs could not be observed in the high-temperature patterns. Thus the appearance of corresponding superstructures was concluded from the few lines with high d values which appeared on heating in the high-temperature X-ray experiments. The X-ray results show no systematic indication of the existence of phase 5 and of its decomposition, as found by Miyatani from his experiments and verified in our DSC measurements by the appearance of corresponding effects. However, in some quenched samples (35.6–35.9 mole% Te) annealed at 620–720 K, a new phase was found. The powder pattern could be indexed with a monoclinic unit cell a = 8.73 Å, b = 14.600 Å, c = 7.199 Å, β = 90.33° which is a monoclinic distortion of phase 4. The transformation temperatures observed between 34.9 and 35.3 mole% Te are in very good agreement with the temperatures reported by Mills *et al.* (*15*), who used a

sample with 35.3 mole% Te for the determination of the specific heat of Cu_2Te. The only transition which could be observed in the high-temperature X-ray experiments in this concentration range was that corresponding to the appearance of the simple hexagonal phase 8.

Between 33.5 and 34.9 mole% Te two room-temperature phases were found. The phase at 33.63 mole% Te probably has an orthorhombic lattice (a = 7.319 Å, b = 22.236 Å, and c = 36.458 Å, phase 1) in agreement with the results of Baranova (*12*). An indexation of the results was also possible with a triclinic distorted hexagonal lattice of the Nowotny phase $a' = c_N \sim 7.24$, $b' = 2c_N \sim 14.50$, $c' = a_N \sim 4.23$; $\alpha \sim 92.2$, $\beta \sim 92.1$, $\gamma \sim 83.8$). The second orthorhombic phase between 34.4 and 34.9 mole% Te (phase 2) has lattice parameters of a = 10.186 Å, b = 10.308 Å, and c = 4.234 Å; this lattice is related to the $Cu_{1.94}Te$ phase of Stevels ($a \sim a_{st} \cdot \sqrt{2}$, $b \sim c_{st} \cdot \sqrt{2}$, $c \sim b_{st}$).

In high-temperature X-ray studies of the phases 2 and 1, no effect could be observed at 450 K (DSC peak), whereas at ~600 K a new phase with hexagonal symmetry and a = 8.53 Å, c = 36.03 Å (phase 7) appeared. In addition, in the measurements of phase 1, a new phase (6), stable between 550 and 590 K, was observed. The thermal effects of the 33.63% sample were identical to the effects observed by Kubaschewski and Nölting (*16*) in an adiabatic Cp measurement of Cu_2Te (33.5 mole% Te). Deviations in the results of Mills and the latter authors are thus the result of the different chemical composition of their samples.

Above 635 K the different superstructures of $Cu_{2-x}Te$ transform into a hexagonal phase with a broad homogeneity range (phase 8, 33.3–36.0 mole% Te). The X-ray pattern agrees well with a phase observed by Nowotny. The unit cells vary linearly from a = 4.25 Å, c = 7.33 Å (33.3 mole% Te) to a = 4.19 Å, c = 7.29 Å (36.1 mole% Te). With increasing temperature this hexagonal solid solution changes into a cubic solid solution (phase 9), the transformation temperatures as well as the lattice parameters depending on the tellurium concentration. A phase similar to phase 8 was obtained from the $Cu_{2-x}Te$ phases in the grinding experiments. The phase diagram for $Cu_{2-x}Te$ constructed from the DSC effects of ground samples is simple (Fig. 5).

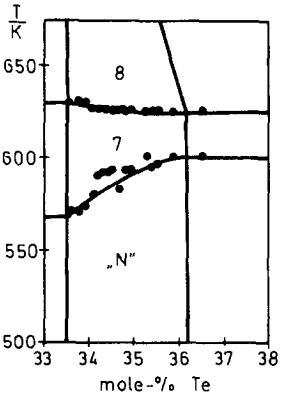

FIG. 5. Possible phase diagram of $Cu_{2-x}Te$ after grinding.

Within the region of higher Te concentration another phase exists with the composition $Cu_{3-x}Te_2$ (Figs. 2, 3). The homogeneity range of the orthorhombic phase was found by X-ray and DTA measurements to lie between 40.0 and 41.1 mole% Te. Thus the homogeneity range is smaller than that found by other authors, though this result is supported by experiments of Mizota (*17*). The high-temperature behavior of this phase was also studied by Anderko and Schubert (*3*), and most recently by Stevels (*6*) and Stevels and Wiegers (*18*).

According to the abovementioned authors, the tetragonal form of $Cu_{3-x}Te_2$ persists up to 625 K. Earlier observations by Anderko (*3*) and Burmeister (*19*) have shown that the homogeneity range of the $Cu_{3-x}Te_2$ phase shifts to higher copper concentrations with increasing temperature.

Above 633 K a face-centered cubic structure was observed by Stevels and Wiegers (*18*), which is not in agreement with Anderko (*3*) or with our results. For concentrations from 36 to 41 mole% Te we observed a phase of unsolved structure. The DTA and X-ray results indicate that this phase is surprisingly stable at temperatures well above the decomposition temperature of rickardite (920 K). The X-ray pattern found at 42 mole% Te is closely related to that of the former phase. However, in high-temperature X-ray experiments this phase decomposes at 920 K. The high-temperature phase region of rickardite may therefore include two phases with similar structures but different thermal stabilities as shown in Fig. 3.

At 400°C, the occurrence of two new phases is also indicated by coulometric titration experiments performed by Lorenz and Wagner (*20*). According to studies

TABLE I

X-RAY POWDER DATA OF Cu–Te PHASES[a]

Phase 4				Phase 3			
d_{obs}	d_{calc}	hkl_{hex}	I_{est}	d_{obs}	d_{calc}	hkl_{hex}	I_{est}
7.200	7.22	001	w	10.68	10.87	001	vw
	7.21	100		5.41	5.438	002	vw
4.15	4.16	110	vw	3.628	3.627	200	vs
3.612	3.610	002	vs		3.625	003	
	3.606	111		3.244	3.243	103	
	3.605	200		3.105	3.108	202	
3.229	3.228	102	s	2.785	—	—	w
	3.225	201		2.563	2.564	203	w
2.730	2.727	112	m	2.361	2.361	301	m
	2.725	210		2.177	2.176	204	m
2.551	2.551	202	w	2.084	2.094	220	s
	2.549	111			2.084	005	
2.282	2.283	103	m	2.011	2.012	310	s
	2.280	301			2.012	303	
2.175	2.175	212	w	1.955	1.955	222	m
2.084	2.084	113	s	1.814	1.814	400	m
	2.081	220			1.814	223	
2.000	2.001	203	s		1.813	006	
	2.001	302		1.760	1.760	313	w
	2.000	221			1.760	106	
	2.000	310		1.623	1.622	403	w
1.804	1.805	003	m		1.621	206	
	1.804	213		1.567	1.567	411	w
	1.803	222		1.451	1.451	500	w
	1.802	400			1.451	413	
1.751	1.751	104	w		1.451	306	
	1.749	312					
	1.749	401					
1.613	1.614	204	w				
	1.613	402					
	1.612	321					
1.364	1.364	115	w				
	1.364	224					
	1.363	323					
1.340	1.340	205	w				
	1.340	314					
	1.349	502					

TABLE I—*Continued*

Phase 5				Phase 2′			
d_{exp}	d_{calc}	hkl	I_{est}	d_{obs}	d_{calc}	hkl	I_{est}
7.258	7.263	−110	vw	7.21	7.245	110	w
5.46	5.470	−101	vw	3.656	3.656	111	s
3.632	3.631	−220	s	3.623	3.623	220	s
3.609	3.609	201	s	3.397	3.395	300	w
3.248	3.248	−221	s	3.272	3.272	021	m
3.228	3.228	−112	s	3.255	3.255	130	s
3.015	3.015	−122	w			201	
2.727	2.729	132	w	3.224	3.225	310	m
2.565	2.566	241	m	3.189	—	—	(phase 1)
	2.566	−311	m	2.756	2.753	221	w
2.555	2.556	311	m	2.580	2.581	131	vw
2.548	2.548	222	m	2.564	2.565	311	vw
2.358	2.364	013	m	2.546	2.547	400	vw
2.282	2.279	−113	m	2.144	—	—	(phase 1)
2.174	2.174	312	m	2.117	2.117	002	m
2.094	2.093	400	s	2.099	2.098	331	s
2.081	2.080	133	s	2.020	2.021	241	s
2.010	2.012	−420	s			150	
1.998	1.996	223	s	2.009	2.010	421	s
				1.842	1.842	431	m
				1.828	1.828	222	m
				1.808	1.808	511	m

Phase 1		HT-Rickardit II	
d_{exp}	I_{est}	d_{exp}	I_{est}
7.230	m	3.60	m
3.706	vw	3.43	m
3.650	w	3.30	m
3.617	w	3.27	m
3.592	m	3.12	m
3.409	s	2.90	s
3.258	s	2.08	m
3.223	w	2.02	s
3.181	s	2.015	m
2.694	w	1.99	m
2.580	w		
2.476	w		
2.144	vs		
2.116	s		
2.097	vs		
2.055	w		
2.017	vw		
2.009	m		

[a] The unit cells were calculated from the powder patterns by the program ITO, developed by Visser (*22*).

made by these authors, three phases exist at 400°C with homogeneity ranges from 33.3 to 34.5 mole% Te (Cu_2Te), 41.2 to 41.8 mole% Te (high-temperature rickardite I?) and 43.1 to 43.5 mole% Te (high-temperature rickardite II?). In electron diffraction studies the low temperature $Cu_{3-x}Te_2$ phase reveals a very complicated behavior with a variety of superstructures, similar to the results found for $Cu_{2-x}Te$ (*21*). These different superstrucutres were not observed by DSC and normal X-ray methods.

The identification of the phase relations in the $Cu_{3-x}Te_2$ region was seriously hampered by experimental difficulties. In the range from 37.5 to 42 mole% Te a phase separation was observed. The samples consist of two layers of grey (Cu_2Te) and violet color ($Cu_{3-x}Te_2$) with a relatively sharp phase boundary, though no other indications for the occurence of a miscibility gap could be found. The demixing leads to a very slow equilibration of the samples. After annealing for 6 months at 770 K samples in this region still consists of CuTe, $Cu_{3-x}Te_2$, and Cu_2Te. The preliminary Cu–Te phase diagram presented in this paper and in other papers and the X-ray powder data given in Table I must be viewed in the light of these difficulties and of those reported for the $Cu_{2-x}Te$ results.

Acknowledgments

We express our gratitude to the Deutsche Forschungsgemeinschaft and the Fonds der Chemischen Industrie who supported this work.

References

1. M. HANSEN AND K. ANDERKO, "Constitution of Binary Alloys," p. 638, McGraw–Hill, New York (1958).
2. K. SCHUBERT, K. ANDERKO, M. KLUGE, H. BUSKOW, E. DÖRRE, AND P. ESSL, *Naturwiss.* **40,** 269 (1953).
3. K. ANDERKO AND K. SCHUBERT, *Z. Metallkd.* **45,** 371 (1954).
4. I. PATZAK, *Z. Metallkd.* **47,** 418 (1956).
5. KIEU VAN CON AND H. RODOT, *C.R. Acad. Sci. Paris* **260,** 1908 (1965).
6. A. L. N. STEVELS, *Philips Res. Rep. Suppl.* 1969 No 9, 1.
7. S. MIYATANI, S. MORI, AND M. YANAGIHARA, *J. Phys. Soc. Japan* **47,** 1152 (1979).
8. B. GATHER, Thesis, T. U. Clausthal, 1974.
9. H. NOWOTNY, *Z. Metallkd.* **37,** 40 (1946).
10. B. P. BURYLEV, N. N. FEDOROVA, AND L. SH. TSEMEKHMAN, *Russ. J. Inorg. Chem.* **19,** 1249 (1974).
11. R. V. BARANOVA AND Z. G. PINSKER, *Russ. J. Strukt. Chem.* **11,** 637 (1970).
12. R. V. BARANOVA, V. P. AREF'EV, AND S. A. SEMELITOV, *Inorg. Mater.* **13,** 1720 (1977).
13. F. GUASTAVINO, H. LUGUET, AND J. BOUGNOT, *Mater. Res. Bull.* **8,** 835 (1973).
14. M. I. TSYPIN AND A. A. CHIPIZHENKO, *Inorg. Mater.* **10,** 1037 (1974).
15. K. C. MILLS AND M. J. RICHARDSON, *Thermochim. Acta* **6,** 427 (1973).
16. P. KUBASCHEWSKI AND J. NÖLTING, *Ber. Bunsenges Ges.* **77,** 70 (1973).
17. T. MIZOTA, K. KOTO, AND N. MORIMOTO, *Mineral. J.* **7,** 252 (1973).
18. A. L. N. STEVELS AND G. A. WIEGERS, *Recl. Trav. Chim. Pay-Bas* **90,** 352 (1971).
19. J. BURMEISTER, *Z. Metallkd.* **57,** 325 (1966).
20. G. LORENZ AND C. WAGNER, *J. Chem. Phys.* **26,** 1607 (1957).
21. D. COLAITIS, D. VAN DYCK, P. DELAVIGNETTE, AND S. AMELINCKX, *Phys. Status Solidi* A **58,** 271 (1980).
22. J. W. VISSER, *J. Appl. Crystallogr.* **2,** 89 (1969).